bioRxiv preprint doi: https://doi.org/10.1101/642272; this version posted September 18, 2019. The copyright holder for this preprint (which was not certified by peer review) is the author/funder, who has granted bioRxiv a license to display the preprint in perpetuity. It is made available under aCC-BY-NC-ND 4.0 International license.

Title: Force-based assessment distinguishes between the age-related and post-stroke changes in the neural control of reaching.

Authors: Ariel B. Thomas[1,2], Erienne V. Olesh[1,2], Amelia Adcock[3,4], and Valeriya Gritsenko[1,2]

Affiliations:

[1] Department of Human Performance, Division of Physical Therapy, School of Medicine West Virginia University, Morgantown, WV, 26506

[2] Rockefeller Neuroscience Institute, Department of Neuroscience, West Virginia University, Morgantown, WV, 26506

[3] WVU Center for Teleneurology and Telestroke, Morgantown, WV, 26506

[4] Department of Neurology, School of Medicine, West Virginia University, Morgantown, WV, 26506

Corresponding author: Valeriya Gritsenko, PO Box 9226, One Medical Center Drive, Morgantown, WV, 26505-9226. Phone: (304) 293-7719

Running Head: dynamic assessment of post-stroke reaching

bioRxiv preprint doi: https://doi.org/10.1101/642272; this version posted September 18, 2019. The copyright holder for this preprint (which was not certified by peer review) is the author/funder, who has granted bioRxiv a license to display the preprint in perpetuity. It is made available under aCC-BY-NC-ND 4.0 International license.

Abstract

Background and Purpose: The way we move changes throughout our lifetime and often we move less as we age. Distinguishing the motor deficits caused by a stroke from changes in motion due to normal aging is important for the accurate assessment of post-stroke recovery and to determine the effectiveness of treatment. The whole repertoire of complex human motion is enabled by forces applied by our muscles and controlled by the nervous system. However, the current medical standard for assessing motor deficits is based on quantifying movement, without a comprehensive analysis of the active forces that cause this movement. The objective here is to estimate active muscle forces from the quantitative recording of motion.

Methods: The motion of twenty-two people was captured when reaching to virtual targets in a center-out task. Eight of the participants had chronic hemiparesis after a stroke, and another six participants were of similar age to the stroke participants. All participants served as their own controls. We used inverse dynamic analysis to derive muscle moments, which were the result of the neural control signals to muscles and caused the recorded multijointed movements. These muscle moments were separated into forces that were related only to movement production from those only related to posture maintenance against gravity. We then compared these muscle forces between limbs to assess how stroke in one hemisphere disrupts the control signals in individuals with hemiparesis compared to the young and age-matched individuals.

Results: We show that both aging and stroke causes the control signals from dominant and non-dominant hemispheres to be less symmetrical in a pattern that indicates worsening neural control of intersegmental dynamics. We also show that the force-based assessment provides consistently higher quality measures of individual motor deficits due to stroke compared to traditional motion-based assessment. Using the force-based assessment, but not motion-based assessment, it was possible to distinguish the motor deficits due to stroke from age-related movement variability.

Conclusions: The results of our study show that it is feasible to distinguish between age-related and stroke-related deficits in the neural control of reaching using inverse dynamic analysis of motion. This is useful for objective home-based monitoring using wearable and mobile devices of patients recovering from a stroke and elderly people at risk of disability. Our results further indicate that the disruption of the neural control of intersegmental dynamics contributes not only to motor deficits after stroke but also to the inefficiency of movement in the elderly.

Keywords: Neuromechanics, Paresis, Nonlinear Dynamics, Muscle Moment, Motor Control, Motor Assessment

bioRxiv preprint doi: https://doi.org/10.1101/642272; this version posted September 18, 2019. The copyright holder for this preprint (which was not certified by peer review) is the author/funder, who has granted bioRxiv a license to display the preprint in perpetuity. It is made available under aCC-BY-NC-ND 4.0 International license.

Introduction

Movement is a complex interplay between forces generated by our muscles under the control of the central nervous system and the environment. When aging or neurological diseases damage the neuromuscular mechanisms of movement production, this fine interplay is disrupted leading to movement impairment, disability, and inactivity [1]. Stroke is the leading cause of long-term disability in the United States with most stroke survivors experiencing movement deficits that are often accompanied by declining motor function. Some evidence exists that stroke accelerates functional decline due to aging [2]. Inactivity and aging are two of the highest risk factors for stroke. With age, less than 23% of adults in the United States report exercising enough to meet government guidelines for physical activity [3]. Lack of physical activity increases the risk of stroke, so that up to 90% of it could be attributed to risk factors that relate directly or indirectly to the lack of physical activity [3]. Thus, physical inactivity in elderly and motor deficits after neurological disorders are tightly intertwined. This underlies the need to quantify movement with enough precision to be able to distinguish the functional changes with age from the movement deficits due to stroke.

The current gold standard in the assessment of movement deficits is based on experienced medical professionals identifying motion abnormalities that are characteristic of specific disorders [4,5]. Due to the complexity of human body and how gravity and external objects affect its motion, the subjective rating of observed motion cannot capture the subtlety of how that motion was generated by neuromuscular action. It is not always possible to infer from the observation of motion what forces were applied by the muscles to make the arm move, even for a seemingly simple judgement of whether the motion is active or passive. For example, force-based analysis has shown counterintuitively that the elbow and wrist motion of a professional baseball pitcher is more passive compared to the unskilled thrower [6,7]. This indicates that the neural motor control system of skilled throwers is honed to take advantage of the passive interaction forces between the shoulder and elbow joints in order to make the throwing movement more efficient and more powerful. This type of force-based analysis may provide valuable insights into the assessment of differences between motion of young and elderly individuals and between healthy motion and that affected by stroke. Therefore, this study aims to provide this insight by deriving muscle forces from observed movement in individuals with post-stroke motor deficits and in age-matched healthy individuals.

Methods

Participants

Twenty-two human participants were recruited to perform reaching movements to virtual targets with both arms. The participants were divided into three groups, Control, Stroke, and Age-matched. The Control group (23 ± 0.5 years) included 8 participants without any known neurological or musculoskeletal disorders (data was reported in Olesh et al.[8]). The Stroke group included 8 participants (54 ± 14 years), who have suffered single unilateral ischemic stroke at least three months prior to the experiment (Table 1). The strokes were diagnosed by neurologists at Ruby Memorial Hospital; the lesion locations were established from medical imaging. Potential participants were excluded if they could not produce visible movement with their shoulder and elbow, or if they were unable to provide written consent to participate. The Age-matched group

bioRxiv preprint doi: https://doi.org/10.1101/642272; this version posted September 18, 2019. The copyright holder for this preprint (which was not certified by peer review) is the author/funder, who has granted bioRxiv a license to display the preprint in perpetuity. It is made available under aCC-BY-NC-ND 4.0 International license.

(52 ± 15 years) included 6 participants without any known neurological or musculoskeletal disorders, whose age was within the mean ± SD of participants in the Stroke group. All participants were right-hand dominant and reported no unrelated movement disorders or significant injuries to their upper extremities. The study and the consent procedure were approved by the Institutional Review Board of West Virginia University (Protocol # 1311129283). All participants provided written consent before participation.

Table 1. Stroke group information.

ID	Gender	Infarct hemi-sphere	Infarct description and location	Age	Years post stroke	Contralateral reach duration (s)
1	F	Left	Left middle cerebral artery	51	3	0.7 ± 0.13
2	M	Left	Left caudate lenticular nuclei and external horn of the left ventricle	58	5	0.8 ± 0.14
3	M	Right	Right dorsal pontine-medullary lacunar infarction	67	0.5	0.7 ± 0.17
4	M	Right	Lacunar infarct in posterior right putamen and border of right internal capsule	68	0.25	0.6 ± 0.09
5	M	Right	Right middle cerebral artery	23	11	0.7 ± 0.19
6	M	Right	Right middle cerebral artery	60	6	0.6 ± 0.12
7	M	Right	Right middle cerebral artery, extending posteriorly	53	7	0.5 ± 0.17
8	M	Right	Right lateral medullary infarction with occluded right vertebral artery	51	8	1.8 ± 0.55

Experimental Task

During the experiment, participants reached to virtual targets in a center-out task, as described in detail in Olesh et al. [8] (Fig. 1). Movements were instructed using a virtual reality (VR) software (Vizard by Wolrdviz) and headset (Oculus Rift), which randomly displayed one of 14 targets, 5 cm in diameter, arranged equidistantly from a center target. A center target was placed in the VR space so that initial arm posture was at 0◦ shoulder flexion, 90◦ elbow flexion, and a 0◦ wrist flexion (Fig. 1A). For each participant, the distance from the center target to the peripheral targets was scaled to 30% of arm length (anterior acromial point to the distal tip of the index finger). This distance between the central and peripheral targets was on average 20 cm. Our most impaired participant (S8, Table 1) was unable to reach targets reliably with his left arm that was contralateral to stroked hemisphere. Therefore, the reaching distance for this participant was decreased to 15 cm.

Participants were seated and instructed to reach to targets as quickly and as accurately as possible without moving their torso. Participants were able to see their arm in real time visualized

bioRxiv preprint doi: https://doi.org/10.1101/642272; this version posted September 18, 2019. The copyright holder for this preprint (which was not certified by peer review) is the author/funder, who has granted bioRxiv a license to display the preprint in perpetuity. It is made available under aCC-BY-NC-ND 4.0 International license.

in VR by a "stick figure" connecting marker positions. Index fingertip was shown as a yellow ball, participants were instructed to move it into the center of each target. Individual joint motion of the digits was not tracked; therefore all participants were instructed to keep palm flat with all fingers extended and wrist pronated (palm down). Participants with stroke wore a finger splint to keep the digits 2-5 extended.

Each movement began with the participant's hand in the center target. A movement was cued by the changing of the color of center target from green to red and the appearance of one peripheral green target (Fig. 1B). Upon the detection of index fingertip inside the peripheral target radius, its color changed to red, cueing the participant to return to the central target (Fig. 1A, end of center-out movement). After the participant reached the center target ((Fig. 1A, end of return movement), the task reset, peripheral target disappeared, and a new one appeared after a half-a-second delay. Movements to each peripheral target location were performed in a randomized order and repeated 15 times with rest breaks after bouts of 70 trials or upon request. Each participant repeated this experiment with both arms in separate sessions.

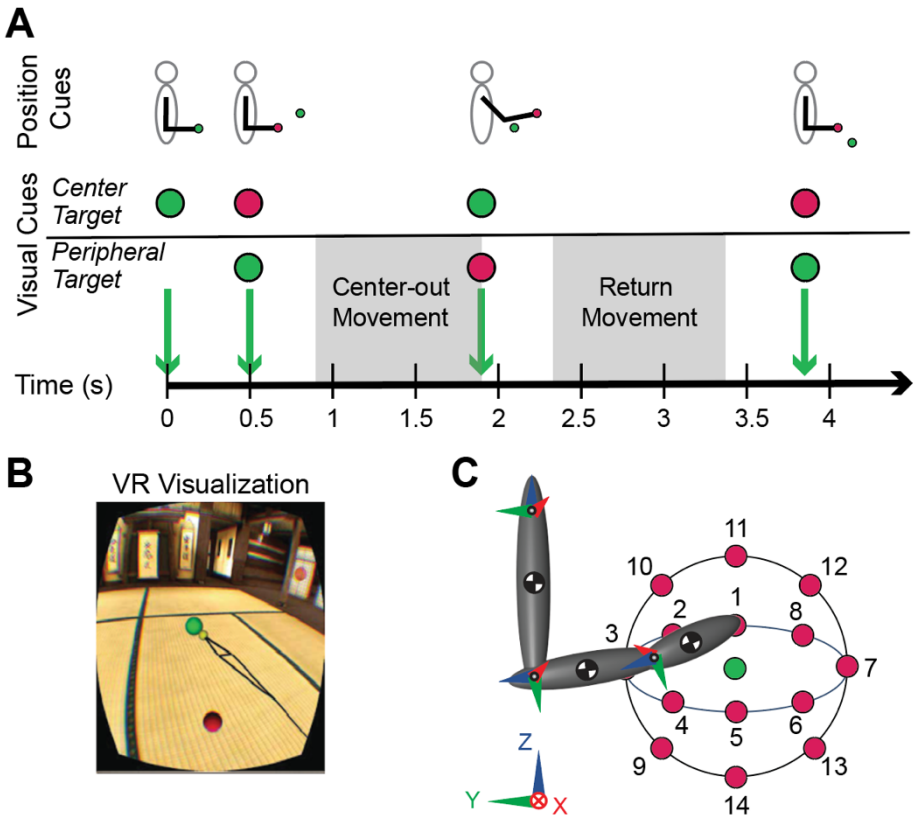

Figure 1. Standardized reaching in virtual reality. A) Trial timeline for each center-out and return reaching movement toward one of 14 peripheral targets. B) Participant's VR view of the targets with visual feedback of their limb position (black stick figure indicating hand, forearm, and upper arm) including fingertip (yellow sphere). C) Side view of the scaled dynamic model of the arm for one participant and relative target locations. The checkered circles represent the centers of mass of the segments. Arrows represent the orientations of local and world coordinate systems used for defining joint angles and degrees of freedom. Shoulder, elbow, and wrist flexion/extension degrees of freedom were calculated around X (red) axes. Shoulder abduction/adduction degree of freedom was calculated around Y (green) axis. Shoulder internal/external rotation degree of freedom was calculated around Z (blue) axis. The relative target

bioRxiv preprint doi: https://doi.org/10.1101/642272; this version posted September 18, 2019. The copyright holder for this preprint (which was not certified by peer review) is the author/funder, who has granted bioRxiv a license to display the preprint in perpetuity. It is made available under aCC-BY-NC-ND 4.0 International license.

locations are shown for all movement directions. The model posture shows a moment in time during the dynamic simulation of a reaching movement from the center target to the peripheral target 11 (movement up).

Data Collection and Processing

Motion capture was recorded during the experiment using an active-marker motion capture system (Impulse by PhaseSpace) and processed in MATLAB (Mathworks Inc.). The light emitting diodes (active markers, LEDs) were placed according to best practice guidelines on anatomical bony landmarks of the arm and trunk [9]. Motion capture data were collected at a rate of 480 frames per second, low pass filtered at 10 Hz and interpolated with a cubic spline (maximum interpolated gap: 0.2 s). Joint angles were calculated from motion capture using local coordinate systems defined as follows. Six LEDs on the clavicle, sternum, spine and the shoulder of the analyzed arm were used to define the trunk coordinate system. Three LEDs, 2 on the shoulder and 1 on the elbow, were used to define upper arm coordinate system. Three LEDs, 1 on the elbow and 2 on the wrist, were used to define forearm coordinate system. Three LEDs, 2 on the wrist and 1 on the fingertip, were used to define hand coordinate system. The axes of the local coordinate systems were oriented in the same direction for both arms as shown in Fig. 1C. Joint angles were defined as Euler angles that corresponded to five joint degrees of freedom (DOFs) including 3 shoulder DOFs flexion/extension, abduction/adduction, internal/external rotation, 1 elbow DOF flexion/extension, and 1 wrist DOF flexion/extension. In some participants the medial wrist LED was not reliably tracked due to being obscured frequently from camera view by moving body segments. Therefore, wrist pronation/supination DOF was not reliably detected and, thus, excluded from analysis. Wrist abduction/adduction was found to be minimal during these tasks and was likewise not included in the analysis.

The onset and offset of each center-out and return movements were identified from the differentiated trajectory of hand marker (velocity) crossing the threshold of 5% of maximal velocity at the beginning and the end of a given movement. These events were verified through visual inspection of the plotted trajectories to correct for unintended motion around the center target and/or corrective movements around the peripheral target. The onset and offset events were used for temporal normalization of kinematic and dynamic profiles prior to averaging. Signals starting 100 ms prior to the onset events were included in the analysis of each movement to capture the full profile of phase-advanced torques.

Inverse Dynamics

The arm model was implemented in Simulink (Mathworks Inc) and used to calculate forces at the shoulder, elbow, and wrist joints. Joint angles for the shoulder, elbow, and wrist, obtained as described above were used to drive the model and simulate the center-out and return movements. The trunk was assumed to be stationary and in line with the world coordinate system (Fig. 1C). The inertia of major limb segments (humerus, radius/ulna, and hand) were modeled as ellipsoids with the long axes and masses scaled to the lengths of individual participants [10]. Inverse dynamics simulations using the individually-scaled model shown in Fig. 1C were ran in Simbody (Mathworks Inc.) to obtain active muscle torques as described in Olesh et al. [8].

Active muscle torques obtained with inverse simulations were divided into two additive components, termed postural and dynamic forces. The postural forces captured the portion of muscle torque that supports the limb segments against the force of gravity; it can also be thought of as the postural component of forces produced by muscles. The dynamic forces captured the

bioRxiv preprint doi: https://doi.org/10.1101/642272; this version posted September 18, 2019. The copyright holder for this preprint (which was not certified by peer review) is the author/funder, who has granted bioRxiv a license to display the preprint in perpetuity. It is made available under aCC-BY-NC-ND 4.0 International license.

residual muscle torques related to motion production [11,12]. This component can also be through of as the muscle force that would produce the same motion in absence of gravity, e.g. in a microgravity environment. As described in Olesh et al.[8], to obtain the dynamic torque components we ran the inverse dynamics simulations with gravity of the physics engine set to zero. To obtain the postural component, the dynamic torque component was subtracted from the overall active muscle torque obtained from simulations with standard gravity for each DOF.

Statistical Analysis

All statistical analyses were performed in MATLAB. Angular kinematic and torque signals were normalized in time using onsets and offsets of each movement, resampled to 1000 samples, and averaged. Inter-trial variability was calculated as the standard deviation across repetitions of individual movements toward the same target and averaged over the normalized trajectory samples (n = 15). The individual normalized trajectories were averaged to create a mean signal for each center-out and return movement toward each target for each participant. Peak-to-peak values of the mean trajectories and their inter-trial variance are reported in the Supplementary Tables with standard deviations of each measure across participants for each signal type per limb.

The symmetry of motion between right and left limbs was quantified using the interlimb shared variance metric. In this analysis, the participants served as their own controls, which reduced the variability of all measures across them. This enabled the distinction between the effects of aging and stroke on the quality of reaching movement. To obtain the interlimb shared variance metric, the normalized mean trajectories of joint angles and muscle forces were compared between right and left limbs of each participant. The coefficient of determination (R^2) was calculated for each movement direction between the trajectories for the corresponding signals from the right and left limbs of the same participant. These values were then averaged across movement directions for each DOF for each participant. The resulting metric ranged between 0 (low symmetry or high asymmetry) and 1 (high symmetry or low asymmetry).

To test the null hypotheses that the movements of participants in different groups were equally symmetrical, we applied repeated measures analysis of variance (ANOVA) to interlimb shared variance metric for each signal type, i.e. angular kinematics (Table 2), muscle torque (Table 3), postural forces (Table 4), and dynamic forces (Table 5). All four ANOVAs were structured the same way with a single between-subject factor Group with 3 levels (Control, Age-Matched, and Stroke) and two within-subject factors Direction with 28 levels (14 center-out movements to peripheral targets and 14 return movements numbered as in Fig. 1C) and DOF with 5 levels (3 shoulder DOFs flexion/extension, abduction/adduction, internal/external rotation, 1 elbow DOF flexion/extension, and 1 wrist DOF flexion/extension). The p-values with Greenhouse-Geisser adjustment for sphericity were used to determine significance of main and interaction effects [13]. Post-hoc analyses were conducted using multicompare functions in Matlab based on the ANOVA model.

To compare the sensitivity of angle- and force-based metrics, we used k-means clustering algorithm to classify participants into one of 2 groups, stroke and non-stroke. The data used for clustering was R^2 values from either joint angles or dynamic forces for shoulder DOFs summed across movement directions. Elbow and wrist DOFs were excluded from this analysis based on the ANOVA results on dynamic forces, which showed that the R^2 values for these DOFs were not significantly different between Stroke and Age-matched groups. To identify clusters, we used squared Euclidean distance measure with heuristic approach for cluster center initialization [14]. The

bioRxiv preprint doi: https://doi.org/10.1101/642272; this version posted September 18, 2019. The copyright holder for this preprint (which was not certified by peer review) is the author/funder, who has granted bioRxiv a license to display the preprint in perpetuity. It is made available under aCC-BY-NC-ND 4.0 International license.

reproducibility of cluster assignment was tested by running the algorithm 20 times and reporting the chances of individuals being misclassified into the wrong group.

Results

The reaching movements produced by participants with their right and left limbs were highly symmetrical in the Control group and somewhat less symmetrical in the Age-matched and Stroke groups (Table 2, Group effect; Fig. 2A). These differences were consistent across groups for all movement directions and joint DOFs (Table 2, insignificant interaction). Post-hoc analysis found no significant differences in angular kinematics between the Control and Age-matched groups across all DOFs and movement directions. Across movement directions, the angular kinematics of the wrist was less symmetrical in the Stroke group compared to the Age-matched group ($p = 0.02$) and to the Control group ($p = 0.04$); the angular kinematics of the elbow was less symmetrical in the Stroke group than the Control group ($p = 0.02$; Fig. 2A). Across all DOFs, the angular kinematics was less symmetrical in the Stroke group than in the Age-matched group for several center-out movements ($p_7 = 0.01$ for target 7 in Fig. 1, $p_{10} = 0.01$, $p_{11} = 0.03$, $p_{14} = 0.01$) and two return movements ($p_8 = 0.01$, $p_{13} < 0.01$). The angular kinematics was less symmetrical in the Stroke group than in the Control group for a single center-out movement ($p_7 = 0.02$) and two return movements ($p_2 = 0.01$, $p_{13} < 0.01$).

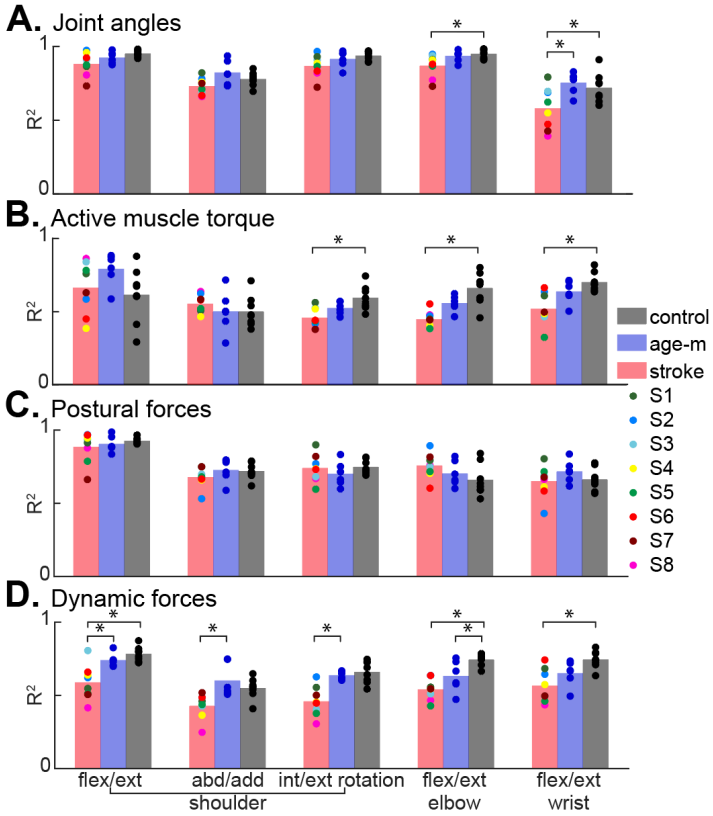

Figure 2. Asymmetry metric. Interlimb shared variance (R^2) is computed between temporal profiles of each limb. Bars show mean R^2 per group (age-m indicates Age-matched group); symbols show values for individual participants. Flexion/extension DOF is abbreviated as flex/ext; abduction/adduction DOF is abbreviated as abd/add; internal/external DOF is abbreviated as int/ext. **A.** Asymmetry based on joint angles. **B.** Asymmetry based on active

bioRxiv preprint doi: https://doi.org/10.1101/642272; this version posted September 18, 2019. The copyright holder for this preprint (which was not certified by peer review) is the author/funder, who has granted bioRxiv a license to display the preprint in perpetuity. It is made available under aCC-BY-NC-ND 4.0 International license.

muscle torque. **C.** Asymmetry based on postural forces (gravity-related component of active muscle torque). **D.** Asymmetry based on dynamic forces (motion-related component of active muscle torque).

Table 2: Repeated measures ANOVA on angular kinematics

Factors	SumSq	DF	MeanSq	F	*p*
Group	60.01	139	0.43	8.89	< 0.01
Within factors	15.62	278	0.06	1.16	0.28
Group * within factors interaction	114.78		0.05	1.00	0.50

SumSq stands for the sum of squares; DF stands for degrees of freedom; MeanSq stands for mean squared error.

These asymmetricities were driven by the changes in the trial-to-trial variability of shoulder motion (Supplementary Table 1). In the Control group, the inter-trial variance of angular kinematics was not different between right and left limbs. In the Age-matched group, left shoulder angles (non-dominant arm) were more variable than the right angles. In contrast, in the Stroke group shoulder angles of the contralateral (hemiparetic) arm were less variable than those of the ipsilateral arm. This is explained by the predominant right hemispheric stroke in our participants, which reduced the movement of the more variable left (non-dominant) arm. This shows that the asymmetry between limbs in the Stroke group is the result of different joint angle trajectories, not inter-trial variability as in the Age-matched group.

The right and left movements appeared much less symmetrical when observed through muscle torques than through joint angles (Fig. 2B). This metric was also more variable across participants in all groups compared to the metric based on joint angles. Across movement directions, post-hoc analysis found no significant differences in muscle torques per DOF between the Control and Age-matched groups, nor between the Stroke and Age-matched groups (Table 3). The muscle torques were less symmetrical in Stroke than in Control group at the shoulder joint for internal/external rotation DOF ($p < 0.01$), at the elbow joint ($p < 0.01$), and at the wrist joint ($p = 0.01$; Fig. 2B). Across all joints, the muscle torques were less symmetrical in the Age-matched group than in the Control group for a single center-out movement ($p_2 < 0.01$). The muscle torques were less symmetrical in the Stroke group than in the Age-matched group for the same and one other center-out movement ($p_2 = 0.04$, $p_8 = 0.01$), and they were less symmetrical in the Stroke group than in the Control group for a single return movement ($p_{13} = 0.04$).

Table 3: Repeated measures ANOVA on active muscle torque

Factors	SumSq	DF	MeanSq	F	*p*
Group	68.36	139	0.49	5.57	< 0.01
Within factors	33.41	278	0.12	1.36	0.13
Group * within factors interaction	208.72		0.09	1	0.5

SumSq stands for the sum of squares; DF stands for degrees of freedom; MeanSq stands for mean squared error.

Movements of non-dominant arm by participants in the Control group were produced by larger muscle torques at most joints with somewhat larger trial-to-trail variability (Supplementary Table 2). This interlimb differences in the amplitude of muscle torques decreased in the Age-matched group and disappeared in the Stroke group (Supplementary Table 2). In the Age-matched

bioRxiv preprint doi: https://doi.org/10.1101/642272; this version posted September 18, 2019. The copyright holder for this preprint (which was not certified by peer review) is the author/funder, who has granted bioRxiv a license to display the preprint in perpetuity. It is made available under aCC-BY-NC-ND 4.0 International license.

group, the muscle torques produced by the left (non-dominant) arm and sometimes the right (dominant) arm decreased compared to young controls, so that the interlimb differences in muscle torque amplitudes were smaller in the Age-matched group (Supplementary Table 2). The reduced muscle torques cannot be accounted for by reduced movement speed; the peak angular velocity was similar between the two limbs in the Age-matched group (Supplementary Table 3). The inter-trial variance of the non-dominant muscle torques was still larger than of the dominant ones (Supplementary Table 2). As expected in the Stroke group, the interlimb differences in muscle torque amplitudes disappeared largely due to decreased amplitude and inter-trial variance of muscle torques in the left (primarily hemiparetic) arm (Supplementary Table 2). This further shows that the asymmetry between limbs in the Stroke and Age-matched groups result from different causes. In the Stroke group the interlimb asymmetry in movement is the result of altered muscle force patterns in the arm contralateral to stroke, while in the Age-matched group the asymmetry is due to increased variability and reduced overall muscle force production in the non-dominant limb.

Forces exerted by muscles during reaching movements quantified as muscle torques were separated into two broad components, postural and dynamic forces (see Methods). We classified postural forces as those needed to overcome gravity, which vary throughout movement as the orientation of limb segments relative to the gravity vector changes. The dynamic forces are those responsible for producing the movement in the absence of gravity and can be thought of as the forces produced by astronauts making the same movement in a microgravity environment.

As with kinematics, we found that the postural forces were less similar between corresponding left and right movements of participants in the Age-matched and Stroke groups compared to young control participants (Fig. 2C; Table 4; Supplementary Table 4). However, the movements appeared more symmetrical when observed through postural forces compared to overall muscle forces (Fig. 2B). Interestingly, the inter-subject variability within the Control group observed in the muscle-force metric is reduced in the postural-force metric. However, across movement directions, post-hoc analysis found no significant differences in postural forces per DOF between groups. Across all joints, no significant differences in postural forces per movement direction were found between the Control and Age-matched groups. The postural forces were less symmetrical in the Stroke group than in the Age-matched group for two center-out movements ($p_3 = 0.03$, $p_5 = 0.02$). The postural forces were less symmetrical in the Stroke group than in the Control group for the same center-out movements ($p_3 = 0.02$, $p_5 = 0.04$) and a return to center movement ($p_1 = 0.02$).

Table 4: Repeated measures ANOVA on postural forces

Factors	**SumSq**	**DF**	**MeanSq**	**F**	***p***
Group	52.46	139	0.38	4.68	< 0.01
Within factors	29.67	278	0.11	1.32	0.14
Group * within factors interaction	190.63		0.08	1	0.5

SumSq stands for the sum of squares; DF stands for degrees of freedom; MeanSq stands for mean squared error.

The differences between groups were the largest and most consistent when observed with the dynamic force metric (Fig. 2D). The movements were progressively less symmetrical between limbs from Control to Age-matched to Stroke groups across all joints and movement directions (Table 5). Across movement directions, post-hoc analysis found that the interlimb asymmetry

bioRxiv preprint doi: https://doi.org/10.1101/642272; this version posted September 18, 2019. The copyright holder for this preprint (which was not certified by peer review) is the author/funder, who has granted bioRxiv a license to display the preprint in perpetuity. It is made available under aCC-BY-NC-ND 4.0 International license.

between the Control and Age-matched groups was driven by differences in the profiles of elbow dynamic forces ($p = 0.03$). Between the Control and Stroke groups the interlimb asymmetry was driven by differences in the profiles of shoulder flexion/extension dynamic forces ($p < 0.01$), elbow dynamic forces ($p < 0.01$) and wrist dynamic forces ($p = 0.02$). However, between the Age-matched and Stroke groups the interlimb asymmetry was driven by differences in the profiles of only shoulder dynamic forces (flexion/extension $p < 0.01$, abduction/adduction $p = 0.01$, internal/external rotation $p = 0.01$).

Table 5: Repeated measures ANOVA on dynamic forces.

Factors	SumSq	DF	MeanSq	F	p
Group	66.72	139	0.48	6.76	< 0.01
Within factors	23.35	278	0.08	1.18	0.25
Group * within factors interaction	167.72		0.07	1	0.5

SumSq stands for the sum of squares; DF stands for degrees of freedom; MeanSq stands for mean squared error.

Across DOFs, the interlimb asymmetry between the Control and Age-matched groups was driven by differences in a single return movement that was toward the body ($p_{13} = 0.02$). The interlimb asymmetry between the Stroke and Age-matched groups was driven by differences in movements that were outward away from the body ($p_5 = 0.05$, $p_7 = 0.01$, $p_8 < 0.01$), downward toward the body ($p_9 = 0.03$), and movement up ($p_{11} < 0.01$). The interlimb asymmetry between the Stroke and Control groups was driven by the same outward movements as between the Stroke and Age-matched groups ($p_5 = 0.01$, $p_6 = 0.04$, $p_7 = 0.03$, $p_8 < 0.01$) plus some return to center movements ($p_2 < 0.01$, $p_6 = 0.04$, $p_{13} = 0.01$) and the movement up ($p_{11} < 0.01$). Note that motion asymmetry in Stroke group include both age-related and stroke-related differences between forces produced by left and right limbs. These confounding effects can be separated by the analysis focused on the DOFs that drive asymmetry across multiple movements between Age-matched and Stroke groups (see below the results of clustering).

The inter-trial variance of the dynamic forces was much lower than that of the postural forces or the overall muscle torques (Supplementary Table 5). This increased acuity of dynamic-force assessment enabled us to conclusively determine that both the amplitude and the inter-trial variance of the dynamic forces in the non-dominant arm was consistently larger than that of the dominant arm across all DOFs for both the Control and Age-matched groups (Supplementary Table 5). This suggests that across the lifespan, the motor commands from the non-dominant hemisphere are less energy efficient, requiring more force to make the same motion as that accomplished by the dominant arm. This also shows that in the young, the increased variability due to larger forces of the non-dominant arm is compensated for by the appropriate neural coordination, so that the force trajectories are symmetrical. However, with age this compensation worsens so that even with lower forces due to sarcopenia, the movements are less symmetrical, thus less coordinated.

bioRxiv preprint doi: https://doi.org/10.1101/642272; this version posted September 18, 2019. The copyright holder for this preprint (which was not certified by peer review) is the author/funder, who has granted bioRxiv a license to display the preprint in perpetuity. It is made available under aCC-BY-NC-ND 4.0 International license.

We also found that comparing dynamic forces produced by each limb resulted in a more sensitive measure of individual post-stroke motor deficits than comparing the motion itself, such as joint angles of left and right limbs. Most of the participants in the Stroke group had mild hemiparesis, so that motion with their less-affected ipsilesional arm and hemiparetic contralesional arm were largely symmetrical. This was reflected in high interlimb shared variance between the joint angle profiles in most individuals with stroke (Fig. 3A, joint angles). In contrast, the shared variance between the dynamic torque profiles of the two limbs was much lower in the same participants (Fig. 3A, dynamic forces), indicating a higher degree of motor deficit than what was observed from kinematics.

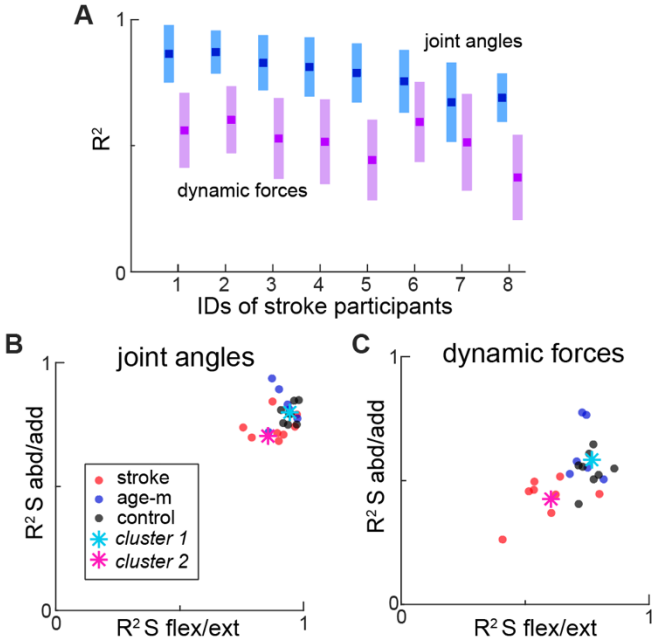

Figure 3. Quantifying movement deficits after stroke using muscle forces is better than that using joint angles. **A.** Interlimb shared variance (R^2) for joint angles and dynamic forces averaged across movement directions. The central tendencies of data per subject are shown as means (dark boxes) with standard deviation (light bars). **B.** & **C.** Clustering results on interlimb R^2 based on joint angles (**C**) and dynamic forces (**D**) averaged across all movement directions.

To investigate how the kinematic and dynamic measures may affect the detection of individual motor deficits due to stroke and the distinction of these deficits from age-related changes in movement, we used k-means clustering analysis (see Methods). Clustering showed a larger separation between Stroke group participants and the rest based on dynamic forces compared to that based on joint angles (Fig. 3B & C). The distance between clusters based on joint angles was 0.18 ± 0.038, while the distance between clusters based on dynamic forces was 0.30 ± 0.003. Consequently, more individuals were misclassified into the wrong group using joint-angle clustering (Stroke: 3 participants were misclassified 19/20 or 20/20 times, 1 participant – 12/20, 2 participants - 8/20, and 2 participants – 1/20; Age-matched: 1 participant – 5/20 and 2 participants – 2/20; Control: 1 participant – 1/20) than using dynamic-force clustering (Stroke: 1 participant was misclassified 16/20 times; Control: 1 participant – 20/20). This shows that the sensitivity and discriminatory power of force-based assessment of motor deficit due to stroke is much higher than motion-based assessment.

bioRxiv preprint doi: https://doi.org/10.1101/642272; this version posted September 18, 2019. The copyright holder for this preprint (which was not certified by peer review) is the author/funder, who has granted bioRxiv a license to display the preprint in perpetuity. It is made available under aCC-BY-NC-ND 4.0 International license.

Discussion

Here we report that age-related changes in the neuromuscular system are most evident in the pattern of forces that accompany movements of non-dominant limb. These age-related changes in the quality of movement present a challenge for the assessment of motor deficits in elderly individuals who have suffered a stroke. The problem is to distinguish between age-related and stroke-related changes in movements in individuals whose pre-stroke state is not known. We propose a possible solution to this problem, which is to assess motion in terms of muscle forces rather than the traditional assessment based on movement kinematics.

Our results indicate that movement of the elderly is less efficient than movement of the young. It is well established that muscle forces decline with age [15]. Consequently, we observed that the peak muscle torques produced during the reaching movements in our experiment were lower in the Age-matched group compared to the Control group. However, this decrease cannot account for the increased interlimb asymmetry pattern we observed in the Age-matched group compared to the Control group. Two facts support this argument. The first fact is that we observed differences in peak muscle torques between the limbs in the Control group without the associated increased interlimb asymmetry. Instead, the muscle torque profiles in the Control group were highly symmetrical between limbs despite differences in peak forces. The second fact is that we normalized the torque profiles to the maximal value across all movement directions for each limb to specifically minimize the contribution of different force magnitudes to the measure of interlimb asymmetry. Despite this normalization, we observed increased asymmetry between the profiles of forces for each limb in Age-matched group compared to the Control group (Fig. 2). Therefore, the increased interlimb asymmetry with age is likely due to the changes in the neural control of movement that affect the pattern of muscle force production and interlimb coordination. The altered pattern of muscle forces results in inefficient movement, which is likely to contribute to slowness [16] and fatigue [17] in the elderly. The majority of identified predictors of inactivity in elderly rely on psychosocial metrics [18,19] that indirectly relate to motor control. Our approach of force-based assessment of motion can be applied on a large scale, opening up new directions of inquiry into the causes of inactivity based on the causal relationship between age-related changes in the nervous and musculoskeletal systems [20] and the resulting movement.

The age-related discoordination in the neural control of movement has characteristic features that can be distinguished from neural control deficits caused by stroke. The prevalent theory of interhemispheric differences in reaching motor control is that the dominant hemisphere is more finely tuned to the control of limb dynamics than the non-dominant hemisphere [21,22]. Specifically, the control of whiplash interaction forces, often referred to as interaction torques that arise during motion of multisegmented limb, is a challenge for the central nervous system [23]. With age, the neural control of interaction torques gets worse [24], which can explain the increased interlimb asymmetry based on dynamic forces in the Age-matched group observed in our study. After a stroke, the control of interaction torques is further disrupted, which is thought to be one of the major causes of the inefficiency of movement in people with hemiparesis [25]. Here we further show that the force-based measures of individual motor deficits are much more sensitive than motion-based measures in quantifying the subtle multijoint differences in complex 3D reaching movements caused by the individual pattern of neural damage due to stroke. We have also found that the force-based measures can be used to disambiguate the age-related deficits from stroke-related deficits so that individuals can be classified reliably into a stroke- or non-stroke group across the lifespan (Fig. 3). A force-based assessment developed based on this method could be

bioRxiv preprint doi: https://doi.org/10.1101/642272; this version posted September 18, 2019. The copyright holder for this preprint (which was not certified by peer review) is the author/funder, who has granted bioRxiv a license to display the preprint in perpetuity. It is made available under aCC-BY-NC-ND 4.0 International license.

helpful in tailoring physical therapy and other rehabilitation programs to the individual. This type of assessment may be especially useful for patients who have less "observable" deficits, such as those classified as asymptomatic via traditional motion-based assessments, but who may still report difficulty moving, increased fatigue and/or inactivity. Technology has advanced to the point where low-cost commercial devices that observe our movement in combination with sophisticated algorithms are becoming widely available for home use. Our study has shown that estimating muscle forces that drive motion can enable a new type of automated assessment of human motor function. This approach can be potentially useful as part of telemedicine and mobile health initiatives, where the patient's health needs to be monitored remotely. Lastly, the analysis of forces that produce movement could also provide a unique insight into the underlying mechanisms of neural and musculoskeletal interactions that will inform future therapies.

Acknowledgments

We thank the study participants for generously giving their time, and M. Powers for her assistance with participant recruitment and the general support of the study; we acknowledge the technical support expertly provided by B. Pollard; we are thankful for insightful and critical comments of S. Yakovenko.

Funding

The study was supported by NIH/NIGMS U54GM104942, T32GM081741, T32AG052375, P20GM109098, and P30GM103503.

References

1. CDC. National Center for Chronic Disease Prevention and Health Promotion, Nutrition D of, Activity P, Obesity. State of West Virginia. Nutrition, Physical Activity, and Obesity Profile. CDC; 2012.

2. Dhamoon MS, Longstreth WT, Bartz TM, Kaplan RC, Elkind MS V. Disability Trajectories Before and After Stroke and Myocardial Infarction: The Cardiovascular Health Study. *JAMA Neurol.* [Internet]. 2017;74:1439–1445. Available from: http://archneur.jamanetwork.com/article.aspx?doi=10.1001/jamaneurol.2017.2802

3. Benjamin EJ, Muntner P, Alonso A, Bittencourt MS, Callaway CW, Carson AP, et al. Heart Disease and Stroke Statistics-2019 Update: A Report From the American Heart Association. *Circulation* [Internet]. 2019;139:e56--e66. Available from: http://eutils.ncbi.nlm.nih.gov/entrez/eutils/elink.fcgi?dbfrom=pubmed&id=30700139&retmode=ref&cmd=prlinks

4. Fugl-Meyer AR, Jaasko L, Leyman I, Olsson S, Steglind S. The post-stroke hemiplegic patient: a method for evaluation of physical performance. *Scand J Rehabil Med*. 1975;7:13–31.

5. Wolf SL, Catlin PA, Ellis M, Archer AL, Morgan B, Piacentino A. Assessing Wolf motor function test as outcome measure for research in patients after stroke. *Stroke* [Internet]. 2001;32:1635–1639. Available from: http://eutils.ncbi.nlm.nih.gov/entrez/eutils/elink.fcgi?dbfrom=pubmed&id=11441212&retmode=ref&cmd=prlinks

6. Gray S, Watts S, Debicki D, Hore J. Comparison of kinematics in skilled and unskilled arms of the same recreational baseball players. *J. Sports Sci.* [Internet]. 2006;24:1183–

bioRxiv preprint doi: https://doi.org/10.1101/642272; this version posted September 18, 2019. The copyright holder for this preprint (which was not certified by peer review) is the author/funder, who has granted bioRxiv a license to display the preprint in perpetuity. It is made available under aCC-BY-NC-ND 4.0 International license.

1194. Available from: http://www.tandfonline.com/doi/abs/10.1080/02640410500497584

7. Hirashima M, Kudo K, Watarai K, Ohtsuki T. Control of 3D limb dynamics in unconstrained overarm throws of different speeds performed by skilled baseball players. *J. Neurophysiol.* [Internet]. 2007;97:680–691. Available from: http://jn.physiology.org/cgi/doi/10.1152/jn.00348.2006

8. Olesh E V, Pollard BS, Gritsenko V. Gravitational and Dynamic Components of Muscle Torque Underlie Tonic and Phasic Muscle Activity during Goal-Directed Reaching. *Front. Hum. Neurosci.* [Internet]. 2017;11:1–12. Available from: https://www.frontiersin.org/article/10.3389/fnhum.2017.00474

9. Robertson G, Caldwell G, Hamill J, Kamen G, Whittlesey S. Research Methods in Biomechanics, 2E [Internet]. Human Kinetics; 2013. Available from: http://books.google.com/books?id=gRn8AAAAQBAJ&printsec=frontcover&dq=intitle:Research+methods+in+biomechanics&hl=&cd=1&source=gbs_api

10. Winter DA. Biomechanics and Motor Control of Human Movement [Internet]. 4th ed. Hoboken, New Jersey: John Wiley & Sons; 2009. Available from: http://books.google.com/books?id=_bFHL08IWfwC&printsec=frontcover&dq=intitle:Biomechanics+and+motor+control+of+human+movement&hl=&cd=1&source=gbs_api

11. Gottlieb GL, Song Q, Almeida G, Hong DA, Corcos D. Directional control of planar human arm movement. *J. Neurophysiol.* [Internet]. 1997;78:2985–2998. Available from: http://eutils.ncbi.nlm.nih.gov/entrez/eutils/elink.fcgi?dbfrom=pubmed&id=9405518&retmode=ref&cmd=prlinks

12. Russo M, D'Andola M, Portone A, Lacquaniti F, D'Avella A. Dimensionality of joint torques and muscle patterns for reaching. *Front. Comput. Neurosci.* [Internet]. 2014;8:1–21. Available from: http://journal.frontiersin.org/article/10.3389/fncom.2014.00024/abstract

13. Geisser S, Greenhouse SW. An Extension of Box's Results on the Use of the Distribution in Multivariate Analysis. *Ann. Math. Stat.* [Internet]. 1958;29:885–891. Available from: https://projecteuclid.org/euclid.aoms/1177706545

14. Arthur D, Vassilvitskii S. K-Means++: the Advantages of Careful Seeding. In: Proc ACM-SIAM symposium on discrete algorithms. 2007.

15. Dutta C, Hadley EC. The significance of sarcopenia in old age. *journals Gerontol. Ser. A, Biol. Sci. Med. Sci.* [Internet]. 1995;50A:1–4. Available from: http://www.ncbi.nlm.nih.gov/sites/entrez?Db=pubmed&Cmd=Retrieve&list_uids=7493199&dopt=abstractplus

16. Salthouse TA. Speed of behavior and its implications for cognition. In: Birren JE, Schaie KW, editors. Handbook of the Psychology of Aging. New York, NY: Van Nostrand Reinhold Co; 1985. p. 400–426.

17. Faulkner JA, Brooks S V, Zerba E. Skeletal muscle weakness and fatigue in old age: underlying mechanisms. *Annu. Rev. Gerontol. Geriatr.* [Internet]. 1990;10:147–166. Available from: http://www.ncbi.nlm.nih.gov/sites/entrez?Db=pubmed&Cmd=Retrieve&list_uids=2102709&dopt=abstractplus

bioRxiv preprint doi: https://doi.org/10.1101/642272; this version posted September 18, 2019. The copyright holder for this preprint (which was not certified by peer review) is the author/funder, who has granted bioRxiv a license to display the preprint in perpetuity. It is made available under aCC-BY-NC-ND 4.0 International license.

18. Rhodes RE, Quinlan A. Predictors of Physical Activity Change Among Adults Using Observational Designs. *Sport. Med.* 2015;45:423–441.

19. Zimmermann E, Ekholm O, Grønbæk M, Curtis T. Predictors of changes in physical activity in a prospective cohort study of the Danish adult population. *Scand. J. Public Health*. 2008;36:235–41.

20. Seidler RD, Bernard JA, Burutolu TB, Fling BW, Gordon MT, Gwin JT, et al. Motor control and aging: Links to age-related brain structural, functional, and biochemical effects. *Neurosci. Biobehav. Rev.* 2010;34:721–733.

21. Sainburg RL, Kalakanis D. Differences in control of limb dynamics during dominant and nondominant arm reaching. *J. Neurophysiol.* 2000;83:2661–75.

22. Schaffer JE, Sainburg RL. Interlimb differences in coordination of unsupported reaching movements. *Neuroscience*. 2017;350:54–64.

23. Ketcham CJ, Dounskaia N V, Stelmach GE. Multijoint movement control: the importance of interactive torques. *Prog. Brain Res.* [Internet]. 2004;143:207–218. Available from: http://www.ncbi.nlm.nih.gov/sites/entrez?db=PubMed&cmd=retrieve&dopt=AbstractPlus&list_uids=14653166

24. Ketcham CJ, Dounskaia N V, Stelmach GE. Age-related differences in the control of multijoint movements. *Motor Control*. 2004;8:422–436.

25. Raj S, Dounskaia N, Clark WW, Sethi A. Effect of Stroke on Joint Control during Reach-to-Grasp: A Preliminary Study. *J. Mot. Behav.* 2019;